PAZ Quality Assessment Summary

Author(s): *Jorge Jorge Ruiz, Juval Cohen*

Task 3 Mission Experts

Approval: *Davide Giudici, Aresys*

Task 3 Lead

Accepted: *Clement Albinet*

EOP-GMQ EDAP Technical Officer

AMENDMENT RECORD SHEET

The Amendment Record Sheet below records the history and issue status of this document.

ISSUE	DATE	REASON
1.0	29/10/2021	First version
2.0	25/01/2022	Revised after receiving comments from ESA

ACRONYMS

AEP	Antenna Elevation Pattern
CR	Corner Reflector
DEM	Digital Elevation Model
ENL	Equivalent Number of Looks
EULA	End User Licence Agreement
FMI	Finnish Meteorological Institute
HS	High Resolution Spotlight
IRF	Impulse Response Function
ISLR	Integrated Side Lobe Ratio
MGD	Multilook Ground Detected
NA	Not Applicable
NESZ	Noise Equivalent Sigma Zero
PSLR	Peak Side Lobe Ration
RD	Reference Document
SAR	Synthetic Aperture Radar
SC	ScanSAR
SL	Spotlight
SM	StripMap
SSC	Single look Slant range Complex
SNAP	SeNtinel Application Platform
SQT	SAR Quality Toolbox
USP	Unique Selling Proposition
UTM	Universal Transverse Mercator

TABLE OF CONTENTS

1. EXECUTIVE SUMMARY

Quality assessment was performed for the PAZ X-band SAR satellite products following the EDAP assessment guidelines. The PAZ spacecraft is based on the TerraSAR-X platform, and it has a total mass of ~1350 kg, 5 m length and 2.4 m diameter. The PAZ mission is a dual-use mission (civil and defence) funded and owned by the Spanish Ministry of Defence and managed by Hisdesat (Hisdesat Servicios Estratégicos, S.A.), a Spanish private communications company.

The assessment presented in this document is divided into two main parts: Documentation review and the assessment of the test datasets. The document review in sections 2.1 - 2.4 includes the assessment of the available PAZ documentation. The grading of these documents is given in columns 1-4 of the maturity matrix shown in section 1.1. Section 2.5 summarizes the evaluation performed by the Finnish Meteorological Institute (FMI) using the test data delivered for the EDAP project. The grading for this is given in the last column of the maturity matrix. Chapter 3 provides more detailed explanations on the methods and the results of the data analysis performed by FMI.

Only the documents in Hisdesat's web page (https://www.hisdesat.es/en/documentos/) were available. Additional documentation with more detailed description of the calibration and validation procedures were thus not provided to the evaluation team. The product information provided through the openly available documentation (RD-1, RD-2) and the products themselves (as metadata) is overall good. The provided product details include the required information, data is easily accessed and processed, and the data are in a standard file format, easily read and understood. Documentation describing the metrological traceability is not available. All relevant characterisation of the SAR system and data is provided, and metadata includes all relevant ancillary information. Documentation about pre-flight and post-launch calibration is minimal.

No additional higher lever (Level 2) products are processed from the PAZ SSC and MGD products. Most of the uncertainty values relevant for SAR are provided in the PAZ documentation, such as the noise equivalent sigma zero (NESZ) and geolocation accuracy. The integrated side lobe ratio (ISLR) and peak side lobe ratio (PSLR) are not directly provided in the documentation, but the alpha coefficient ($\alpha = 0.6$) used in the Hamming window filter is expressed. Theoretical PSLR and ISLR which correspond to the used alpha value were thus used as a reference. Only single uncertainty values for each product type are usually provided in the openly available documentation (RD-2). Pixel-wise uncertainty for the noise level is provided in the metadata. The methods for uncertainty characterization are not documented. Methods describing the impulse response function (IRF) and the geolocation error analyses performed by the data provider are not described. Methods for assessing the radiometric accuracy and NESZ are also not documented in the openly available PAZ documentation.

An independent quality assessment of the essential quality parameters of SAR, such as spatial resolution, PSLR, ISLR, equivalent number of looks (ENL), antenna elevation pattern (AEP) and NESZ was performed by FMI. Representative datasets collected by the PAZ satellite from various test sites, including distributed targets and point targets were used. Data of the ScanSAR (SC), StripMap (SM), Spotlight (SL) and High-Resolution Spotlight (HS) acquisition modes were analysed. The product type of the analysed data was single look slant range complex (SSC) for SM, SL, and HS imaging modes, and multilooked ground detected (MGD) for the SC imaging mode. The measured quality parameters were compared with the corresponding values provided by Hisdesat in the available documentation. The validation was mainly performed using the SAR Quality Toolbox (SQT) dedicated for the assessment of SAR data quality, developed by Aresys (https://www.aresys.it/end-to-end-simulation/). Processing was also tested with the publicly available Sentinel Application Platform (SNAP) toolbox distributed by the European Space Agency (ESA).

The test data quality analysis results were generally in a good agreement with the values provided by Hisdesat, such as the spatial resolution and geolocation accuracy. The measured PSLR and ISLR in azimuth direction were usually in line with the theoretical values, but in range direction they were a few decibels higher. The ENL in the homogenous targets was typically around 1 for SSC data, and close to the number of looks for MGD data. The ENL of the SSC data in rainforests was

smaller than the ideal value, but this might be related to the areas being not ideally homogeneous in the assessed high spatial resolution data of ~0.5-3 m. The NESZ was usually similar of lower (better) than the values provided in the documentation. The Gamma nought backscatter (γ^0) profile along the range direction extracted from the homogeneous rainforest scenes was horizontal, indicating an accurate correction of the AEP by the data provider. The data were successfully processed in SNAP. Based on the available PAZ documentation and our independent data analysis, we generally conclude that the PAZ data are of a good quality, and the available documentation is at a basic level.

1.1   Mission Quality Assessment Matrix

Product Information	Product Generation	Ancillary Information	Uncertainty Characterisation	Validation
Product Details	Sensor Calibration & Characterisation Pre-Flight	Product Flags	Uncertainty Characterisation Method	Reference Data Representativeness
Availability & Accessibility	Sensor Calibration & Characterisation Post-Launch	Ancillary Data	Uncertainty Sources Included	Reference Data Quality
Product Format	Additional Processing		Uncertainty Values Provided	Validation Method
User Documentation			Geolocation Uncertainty	Validation Results
Metrological Traceability Documentation				

Key
Not Assessed
Not Assessable
Basic
Intermediate
Good
Excellent
🔒 Information Not Public

Figure 1 – Mission Product Quality Evaluation Matrix for the PAZ products.

2. MISSION ASSESSMENT OVERVIEW

2.1 Product Information

Product Details	
Product Name	*Product file names contain information on the processing mode (e.g. SSC, MGD), imaging mode, polarization, antenna receive configuration (single or dual), and timing of acquisitions (start and stop).* *Example:* *PAZ1_SAR_SSC_SL_D_SRA_20180924T034217_20180924T034219*
Sensor Name	*PAZ*
Sensor Type	*X-band SAR*
Mission Type	*Single satellite*
Mission Orbit	*Sun Synchronous*
Product Version Number	*v1.2, v1.6*
Product ID	*NA*
Processing level of product	*Level 1b*
Measured Quantity Name	*Radar backscatter*
Measured Quantity Units	*dB*
Stated Measurement Quality	*Radiometric accuracy of 0.3 - 0.63 dB depending on acquisition mode*
Spatial Resolution (range X azimuth) [m]	***ScanSAR MGD***: *16.8-18.2 X 17.7-18.2* ***Stripmap*** *single polarization: 1.1 X 3.01, 150 MHz bandwidth* ***Spotlight*** *single polarization: 1.18 X 1.46, 150 MHz bandwidth* ***HR Spotlight*** *single polarization: 0.6 X 1.05, 300 MHz bandwidth*
Spatial Coverage (range X azimuth) [km]	***ScanSAR***: *100 X 150* ***Stripmap*** *single polarization: 30 X 50* ***Spotlight*** *single polarization: 10 X 10* ***HR Spotlight*** *single polarization: 6-10 X 5 (range size depends on incidence angle)*
Temporal Resolution	*Repeat period of 11 days. Revisit time of up to 70 hours near the equators and up to 35 hours outside latitudes -35 … 35. Maximum of 100 images per day.*
Temporal Coverage	*Launched in February 2018, expected lifetime 7 years*
Point of Contact	***Address***: *Hisdesat Servicios Estratégicos, SA* *Paseo de la Castellana 149, 5th floor.* ***Telephone***: *+34 914490149* ***Email***: *PAZ@hisdesat.es*
Product locator (DOI/URL)	*NA*
Conditions for access and use	*The end user must accept the End User License Agreement (RD-3) provided by Hisdesat.*
Limitations on public access	*NA*
Product Abstract	*NA*

Availability & Accessibility	
Compliant with FAIR principles	*Most of the Fair principles meet, except: Metadata and data include qualified references to other (meta)data.*
Data Management Plan	*A USP tool (RD-2) is available for registered users for data browse and order, including information about the quota of the user. Nevertheless, the USP tool could not be used by the evaluation team, because they had a dynamic IP address, and not a static one.*
Availability Status	*Possibility to use free software (e.g. SNAP) for data processing and analysis.*

Product Format	
Product File Format	*The product is delivered as a zip file containing the main xml-file and folders with the different product components, such as the SAR image raster files, auxiliary raster files and image previews. The SAR image data of the SSC products is in a COSAR (COmplex SAR) file, containing all focused complex SAR data, together with sample validity and position annotation. The SAR image data of the MGD products is embedded in a GeoTIFF raster file.*
Metadata Conventions	*xml*
Analysis Ready Data?	*No*

User Documentation		
Document	*Reference*	*QA4ECV Compliant*
Product Format Specification	*RD-1*	*No*
Product User Guide	*RD-2*	*No*
EULA	*RD-3*	*No*

Metrological Traceability Documentation	
Document Reference	*No*
Traceability Chain / Uncertainty Tree Diagram Available	*No*

2.2   Product Generation

Sensor Calibration & Characterisation – Pre-Flight	
Summary	*All relevant characterisation of a SAR system stated. No documentation about pre-flight calibration procedures.*
References	*RD-1* *RD-2*

Sensor Calibration & Characterisation – Post-Launch	
Summary	*Metadata includes all reasonable aspects. No documentation about post-launch calibration procedures.*
References	*RD-1* *RD-2*

Additional Processing	
Description	*Basic Level-1b products include SSC, MGD, MGD with ellipsoid correction (GEC), and MGD with ellipsoid and terrain correction (EEC). Documentation explains the basic processing methods of these products. No further Level-2 products are offered by the data provider.*
Reference	*RD-1* *RD-2*

2.3   Ancillary Information

Product Flags	
Product Flag Documentation	*RD-1*
Comprehensiveness of Flags	*The product contains many flags, providing comprehensive information about the product.*

Ancillary Data	
Ancillary Data Documentation	*RD-1*
Comprehensiveness of Data	*All the necessary and relevant ancillary data for SAR systems exists. There are no additional ancillary data related to ground conditions at the time of imaging, such as meteorological data.*
Uncertainty Quantified	*No*

2.4   Uncertainty Characterisation

Uncertainty Characterisation Method	
Summary	*While most of the relevant uncertainty values are given in the documentation, the methods used for uncertainty characterization are not documented.*

Reference	*NA*

Uncertainty Sources Included	
Summary	*Documentation gives limited information about the uncertainty sources included in the calibration procedures. Internal calibration of the instrument is performed in standard products. Calibration factor and noise level given in metadata.*
Reference	*RD-1* *RD-2*

Uncertainty Values Provided	
Summary	*Single uncertainty values have been provided for each product type. Information about the noise power is given for each pixel in the metadata of the product. The expected noise equivalent beta nought (NEBN) is annotated over range with azimuth time tags. The noise power can then be deduced when obtaining the calibrated noise corrected sigma nought backscatter.*
Reference	*RD-2*

Geolocation Uncertainty	
Summary	*Pixel localization accuracy is given for each product type separately. The geolocation accuracy has not been provided for the SC products.*
Reference	*RD-2*

2.5 Validation

Validation Activity #1	
Independently Assessed?	Yes
Reference Data Representativeness	
Summary	*Reference measurements assessed are well representative of the satellite measurements, covering a reasonable range of PAZ satellite's measurements. The total number of assessed images is 42, including corner reflector sites for IRF and localization error analysis, as well as low backscatter images from water and desert areas, and images from homogenous targets in Amazonas rainforest and Antarctica glaciers sites for radiometric analyses. The reference datasets enable an assessment of the most essential quality parameters in SAR, such as spatial resolution, geolocation accuracy, PSLR, ISLR, ENL, NESZ and AEP.*
Reference	*Chapter 3*
Reference Data Quality & Suitability	
Summary	*The quality parameters of the reference data were usually given as a single uncertainty value representing each product type and acquisition mode (e.g. SSC, Stripmap).*

Reference	*RD-2*
Validation Method	
Summary	*The methodology assesses the relevant quality parameters in SAR for the reference datasets and compares them with the uncertainty/quality values provided by Hisdesat in the PAZ documentation. The validation was mainly performed using a dedicated SAR quality analysis toolbox, but processing was also tested with the SNAP toolbox.*
Reference	*Chapter 3*
Validation Results	
Summary	*The test data quality analysis results are generally in a good agreement with the values provided by Hisdesat in the available PAZ documentation. The measured spatial resolution in the IRF analyses is close to the values provided by Hisdesat. Geolocation accuracy was according to the provided values. The ENL in the homogenous targets were close to the ideal values. Only for the SSC data from the rainforests the ENL was lower than expected, probably due to the target properties. The measured PSLR and ISLR were usually close to the theoretical values in azimuth direction, but a few decibels higher in the range direction. The NESZ was similar or lower (better) than the values provided by Hisdesat. The AEP has been well corrected for all acquisition modes. The processing in SNAP was successful. Based on our evaluation results and the quality values provided by Hisdesat, we generally conclude that the PAZ data is of good quality.*
Reference	*RD-2* *Chapter 3*

3. DETAILED ASSESSMENT

This chapter provides detailed information on the independent data analysis and assessment performed by FMI using the reference PAZ satellite SSC and MGD SAR datasets. Table 1 shows the date, acquisition mode, polarization, processing mode and version number of the PAZ scenes provided by Hisdesat and used by the evaluation team for assessment purposes within the EDAP activity. Data were collected from various test sites enabling a comprehensive assessment of the most relevant SAR quality metrics, such as spatial resolution, peak side lobe ratio (PSLR), integrated side lobe ratio (ISLR), geolocation accuracy, equivalent number of looks (ENL), noise equivalent sigma zero (NESZ), and antenna elevation pattern (AEP).

The first part of the data was delivered to FMI in May 2020. The version of these data is 1.2. Additional data from the corner reflector (CR) sites of Neustrelitz, Germany, and Rosamond, California, were ordered later, and delivered to FMI during the first half of 2021. The version of these data is 1.6. The data used for assessment includes scenes from distributed homogeneous and low backscatter areas, as well as point target test sites with corner CRs. The homogeneous targets are used for evaluating the ENL and the AEP. The homogeneous test areas include scenes from the Amazonas Rainforest and Antarctica Glacier. Low backscatter targets are used for assessing the NESZ. Low backscatter scenes were acquired from the Pacific Ocean, Michigan Lake, USA, and from the Sahara Desert. The CR test sites used are from Las Tiesas, Spain, Neustrelitz, Germany, and Rosamond, California. An IRF analysis is performed over the CRs, providing quality values for spatial resolution, geolocation accuracy, and the power distribution of the measured radar beam (PSLR and ISLR).

The SAR Quality Toolbox provided by Aresys was used for assessing the above-mentioned metrics. Data was also processed in SNAP version 8.0 for testing the compatibility of PAZ data in SNAP. The measured quality values were evaluated by comparing them to the corresponding quality values provided by Hisdesat in the publicly available documentation. In case no information regarding a certain quality parameter was found in the PAZ documentation, the quality parameter was evaluated based on commonly known standards or calculated theoretical values.

Table 1: All PAZ data products provided by Hisdesat to FMI and included in the data analysis and evaluation.

Test Area	Date	Acquisition mode	Polarization	Processing mode	Version number
Desert, Sahara	20180924	SL	HH/HV	SSC	1.2
	20180913	SL	HH	SSC	1.2
	20181111	SM	VV	SSC	1.2
	20181122	SM	VV	SSC	1.2
Rosamond, California	20210206	SC	HH	MGD	1.6
	20210217	SC	HH	MGD	1.6
	20210228	SC	VV	MGD	1.6
	20210311	SC	VV	MGD	1.6
Neustrelitz, Germany	20200712	HS	HH	SSC	1.2
	20200717	HS	HH	SSC	1.2
	20201229	HS	VV	SSC	1.6
	20210131	HS	VV	SSC	1.6
	20210316	SL	HH	SSC	1.6
	20210327	SL	HH	SSC	1.6
	20210407	SL	VV	SSC	1.6
	20210418	SL	VV	SSC	1.6
	20200329	SM	VV	SSC	1.2
	20200409	SM	HH	SSC	1.2
	20200420	SM	VV	SSC	1.2
	20200501	SM	HH	SSC	1.2
Glacier, Antarctica	20190303	SC	VV	MGD	1.2
	20190423	SC	HH	MGD	1.2
	20180928	SM	VV	SSC	1.2
	20180930	SM	VV	SSC	1.2

Low backscatter, water surfaces	20181025	SC	HH	MGD	1.2
	20181026	HS	HH/HV	SSC	1.2
	20181027	SM	HH/HV	SSC	1.2
	20181025	SM	HV	SSC	1.2
Rainforest, Amazon	20180724	SC	HH	MGD	1.2
	20180917	HS	VV	SSC	1.2
	20180917	SL	HH/VV	SSC	1.2
	20180729	SM	VV	SSC	1.2
	20180829	SM	VV	SSC	1.2
	20190111	SM	HH	SSC	1.2
Las Tiesas, Spain	20181126	HS	HH	SSC	1.2
	20181207	HS	HH	SSC	1.2
	20181218	HS	HH	SSC	1.2
	20190109	HS	HH	SSC	1.2
Mendoza Province, Argentina	20180919	SC	HH	MGD	1.2
	20180925	SC	VV	MGD	1.2
	20181124	SM	HH	SSC	1.2
	20181222	SM	HH	SSC	1.2

3.1   IRF Analysis

The data for the IRF analysis has been acquired over three different locations: Las Tiesas, Murcia, Spain; Neustrelitz Germany, and Rosamond, California, USA. The location of the CRs in Las Tiesas was not shared with the evaluation team, and therefore geolocation accuracy could not be assessed there. However, all other aspects of the IRF-analysis were assessed. The analysis for Neustrelitz and Rosamond included all aspects of the IRF-assessment, including geolocation accuracy assessment.

Data for the IRF-analysis included 4 ScanSAR (SC) acquisitions from Rosamond, 4 Stripmap (SM), 4 Spotlight (SL) and 4 High Resolution Spotlight (HS) acquisitions from Neustrelitz, as well as 4 HS acquisitions from Las Tiesas. The IRF-analysis is performed using the SQT software of Aresys. A screenshot showing an example of an IRF-analysis in the SQT for Neustrelitz is shown in Figure 2. The red points over the SAR image show the location of the reflectors.
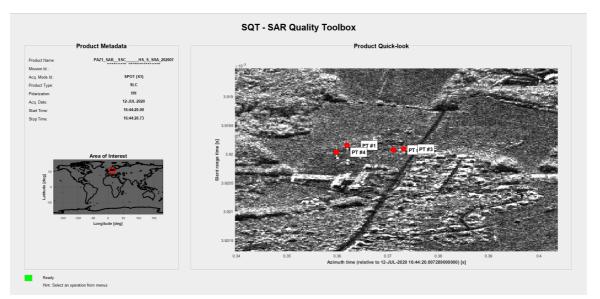

Figure 2: IRF-analysis in Neustrelitz, Germany, using the SQT. The red points show the location of the corner reflectors over the SAR HS image.

The IRF-analysis typically includes an indication of the localization error of a SAR scene. The given locations of the bright targets (CRs) are compared with the location of the reflectors in the SAR

image. The localization error is expressed in both azimuth and range directions. Figure 3 shows an example of the localization error based on one specific CR. The red dot is the expected location of the reflector on the SAR image, based on the geographical coordinates of the reflector (e.g. the true location). The green plus (+) sign shows the location of the same reflector on the SAR image, calculated by the software based on the backscatter distribution.
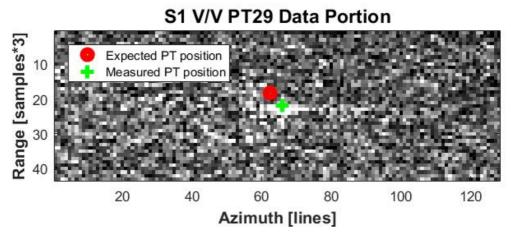

Figure 3: Geolocation accuracy assessment with the SQT. The expected point target (red dot) location is compared with the location in the observed SAR image (green plus sign).

The distribution of the measured power from the reflectors and the area around the reflectors are analysed, providing the spatial resolution of the SAR data and the power of the secondary lobes relative to the main lobe (PSLR and ISLR). Figure 4 shows an example of the spatial distribution of the measured power from one of the CRs in Las Tiesas.
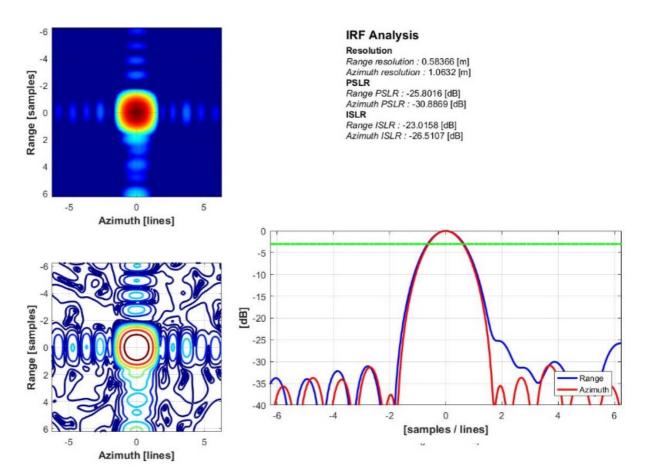
Figure 4. Example of IRF analysis for the HS scene acquired in 7.12.2018 from Las Tiesas, Spain.

The derived IRF-parameters are assessed by comparing them with the values provided in the PAZ-documentation. The evaluation results are therefore considered good if the derived IRF-parameters are better or similar than the values provided by Hisdesat. On the contrary, the quality is considered weak if the derived IRF-parameters are worse than the provided values in the documents. Table 2 shows the IRF-values provided in the PAZ documentation for the single-polarization products. The range spatial resolution is given in slant range direction for SSC, and ground range direction for MGD products.

PSLR and ISLR values have not been directly provided by Hisdesat, but the used alpha coefficient in the applied Hamming window filter was given; α = 0.6. The theoretical PSLR and ISLR for the given alpha value are -31.60 dB and -26.18 dB, respectively. The localization error of the SC mode was also not provided in the documentation. A geolocation uncertainty of 2 m for the standard products due to the accuracy of the GPS orbit determination should be added to the localization error values given in Table 2.

Table 2: Quality values of the test dataset related to IRF-analysis, provided in the PAZ documentation. The theoretical PLSR and ISLR values correspond to the alpha coefficient 0.6 used in the Hamming windowing.

Product type	Range resolution [m]	Azimuth resolution [m]	Localization error [m]	Theoretical PSLR [dB] (α = 0.6)	Theoretical ISLR [dB] (α = 0.6)
ScanSAR MGD	16.79 - 18.19 (45°...20°)	17.66 - 18.18 (45°...20°)	Not provided	-31.60	-26.18

Stripmap SSC	1.76 (100 MHz)	3.01	0.65	-31.60	-26.18
Spotlight SSC	1.18	1.46	0.6	-31.60	-26.18
HR Spotlight SSC	0.6	1.05	0.62	-31.60	-26.18

3.1.1 Las Tiesas

The exact location of the CRs in Las Tiesas was not shared by Hisdesat, and therefore the corners were identified by a visual inspection of the SAR backscatter images. For the HS mode, the CRs were found. However, manual inspection was not successful in finding the CRs used in the Stripmap mode, because of the large size of the images, and because the reflectors were in a different location than in the HS images. For Las Tiesas, the IRF-analysis was thus only performed for the HS scenes.

A total of three CRs were visible on the HS scenes. Due to the lack of exact location information, geolocation errors could not be assessed. However, all other parameters related to IRF-analysis were assessed, namely range and azimuth resolution, PSLR and ISLR. The values depicted in Table 3 are the averages calculated from the three CRs.

Table 3: IRF-analysis results of the HS scenes from Las Tiesas, Spain; ground range and azimuth resolution, PSLR and and ISLR. The table shows the average values calculated from the three corner reflectors.

Image	Range resolution [m]	Azimuth resolution [m]	Range PSLR [dB]	Azimuth PSLR [dB]	Range ISLR [dB]	Azimuth ISLR [dB]
HS_20181126T060328	0.616 ± 0.035	1.112 ± 0.045	-24.689 ± 1.115	-30,876 ± 0.615	-22.066 ± 0.960	-26,496 ± 0.518
HS_20181207T060328	0.583 ± 0.001	1.073 ± 0.041	-25.480 ± 0.620	-31,006 ± 0.182	-22,692 ± 0.462	-26,458 ± 0.080
HS_20181218T060327	0.601 ± 0.020	1.079 ± 0.013	-24.855 ± 0.853	-30,069 ± 1.137	-22,200 ± 0.733	-26,077 ± 0.744
HS_20190109T060326	0.603 ± 0.013	1.135 ± 0.043	-23.090 ± 0.893	-31,717 ± 0.407	-20,971 ± 0.747	-26,452 ± 0,254

The range resolution of the single-pol HS images over Las Tiesas is according to the provided values, while the azimuth spatial resolution slightly worse. Overall, the spatial resolution over the Las Tiesas reflectors is in line with the provided values. The PSLR in range and azimuth directions was around -25 dB and -31 dB, and the ISLR in range and azimuth around -22 dB and -26 dB. The side lobes in the range direction were thus higher than the theoretical values, whereas in azimuth direction they were according to the theoretical values.

3.1.2 Rosamond

Figure 5 shows a Google Earth view of the Rosamond site maintained by NASA's Jet Propulsion Laboratory. The Rosamond site contains several trihedral CRs with face widths of 4.8 m, 2.4 m, and 0.7 m. Most of the reflectors are directed towards the east (descending right looking orbits), including all large (4.8 m), all small (0.7 m) and part of the medium size (2.4 m) reflectors, thus they are visible in the acquired PAZ scenes. The coordinates of the CR locations in the Rosamond calibration site are publicly available through the NASA JPL website: https://uavsar.jpl.nasa.gov/cgi-bin/calibration.pl.

The incidence angle of the SC scenes over the analysed point targets was ~35°, so the ground range and azimuth resolutions according to the definition should be around 17.3 m and 17.8 m, respectively. The measured range and azimuth resolutions of the single-pol SC data over

Rosamond were very similar in all four images. The range resolution was close to 16.6 m, which is somewhat better than the provided value in the documentation, while the azimuth resolution was close to 19.2, which is somewhat worse than the provided value. Overall, the spatial resolution of the data from Rosamond was thus in line with the values provided in the documentation.
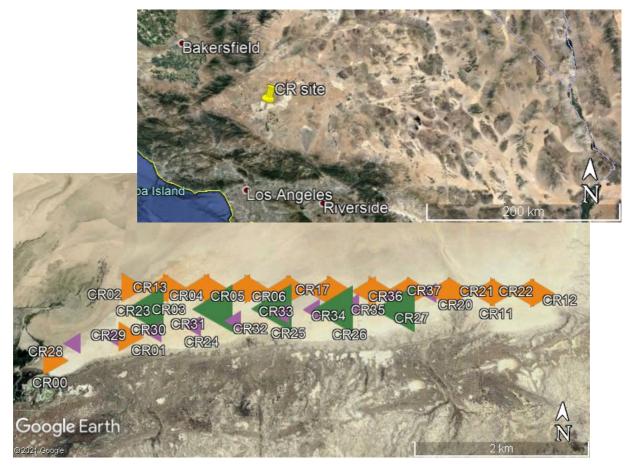

Figure 5: A Google Earth view of the Rosamond CR site in California. The smaller image in the upper right side is a zoom out showing the surrounding area of the CR site. The bottom image is a zoom in on the CR site, showing the CR names, alignment, and distribution at the site.

The localization error was not provided in the documentation for SC data. However, the derived localization error values of ~4.1 m in range and ~3.3 m in azimuth directions indicate good localization accuracy and negligible errors, especially for SC data and when the spatial resolution is larger than the localization error. The PSLR in range and azimuth directions were around -23 dB and -27 dB, and the ISLR in range and azimuth around -18 dB and -21 dB, respectively. The side lobes were thus few decibels higher than the theoretical values calculated for the Hamming window with an alpha coefficient of 0.6 (Table 2).

Table 4: IRF-analysis results of the SC scenes from Rosamond, California; ground range and azimuth resolution, PSLR and ISLR, as well as localization error. The table shows the average values calculated from all corner reflectors.

Image	Range resolution [m]	Azimuth resolution [m]	Range PSLR [dB]	Azimuth PSLR [dB]	Range ISLR [dB]	Azimuth ISLR [dB]	Range Location Error [m]	Azimuth Location Error [m]
SC_20210206T135845	16.634 ± 0.035	19.13 ± 0.135	-23.458 ± 1.486	-26.711 ± 1.578	-18.318 ± 1.259	-21.351 ± 2.457	4.053 ± 0.066	-3.311 ± 0.131

SC_20210217T135844	16.621 ± 0.037	19.198 ± 0.151	-23.423 ± 1.208	-27.415 ± 3.181	-18.102 ± 2.182	-22.072 ± 3.991	4.003 ± 0.058	-3.297 ± 0.088
SC_20210228T135844	16.64 ± 0.035	19.183 ± 0.122	-23.325 ± 2.352	-27.057 ± 4.106	-17.758 ± 3.062	-21.238 ± 4.621	4.142 ± 0.051	-3.372 ± 0.095
SC_20210311T135844	16.625 ± 0.045	19.168 ± 0.209	-23.728 ± 2.341	-25.792 ± 2.743	-17.88 ± 2.316	-19.785 ± 3.253	4.108 ± 0.038	-3.178 ± 0.489

3.1.3 Neustrelitz

Figure 6 shows a Google Earth view of Neustrelitz site. The Neustrelitz site contains 4 trihedral CRs with a face width of 1.5 m. Three of the reflectors; D33, D35 and D36, are directed to the west (ascending right looking orbits) and were therefore visible in the acquired PAZ scenes. The coordinates of the Neustrelitz CR locations are presented in Table 5.

Table 5: Coordinates of the Neustrelitz corner reflectors.

CR name	Latitude (decimal degrees)	Longitude (decimal degrees)	Elevation (m.a.s.l.)
D33	53.32945	13.06939	67
D34	53.33008	13.06963	70
D35	53.33020	13.06952	70
D36	53.32938	13.06991	65

Figure 6: A Google Earth view of the Neustrelitz corner reflector (CR) site in Germany. The small image in the upper right side is a zoom out showing the surrounding area of the CR site. The large image is a zoom in on the CR site, showing the CR names and distribution at the site.

The measured slant range resolution in the Neustrelitz scenes were typically 0.6 m in HS, 1.17 m in SL and 1.75 m, thus very close or even slightly better than the provided values. The measured azimuth resolution in Neustrelitz was typically 1.1 m for HS, 1.6 m for SL and 3.0 m for SM, thus

very similar or slightly coarser than the values provided in the PAZ documentation. Overall, the spatial resolution of the data from Neustrelitz was in line with the values provided in the documentation.

The derived range and azimuth localization errors for Neustrelitz scenes were around 2.5 m and 0.2 m for HS, 2.7 m and 0.3 m for SL, and 2.6 m and 0.2 m for SM, respectively. If taking into consideration the 2 m uncertainty due to the accuracy of the GPS orbit determination together with the values shown in Table 2, these localization errors are in line with the provided error values in the documentation. The PSLR in range and azimuth directions were around -24 dB and -30 dB for HS, -25 dB and -30 dB for SL, and -26 dB and -30 dB for SM, respectively. The derived ISLR in range and azimuth direction were -22 dB and -25 dB for HS, -23 dB and -25 dB for SL, and -24 dB and -25 dB for SM acquisition mode, respectively. The measured PSLR and ISLR in azimuth direction were therefore close to the theoretical values, whereas in the range direction they were somewhat higher than the theorical values.

Table 6: IRF-analysis results of the SM, SL and HS scenes from Neustrelitz, Germany; ground range and azimuth resolution, PSLR and ISLR, as well as localization error. The table shows the average values calculated from all CRs.

Image	Range resolution [m]	Azimuth resolution [m]	Range PSLR [dB]	Azimuth PSLR [dB]	Range ISLR [dB]	Azimuth ISLR [dB]	Range Location Error [m]	Azimuth Location Error [m]
HS_20200712T164420	0.583 ± 0.001	1.067 ± 0.001	-25.827 ± 0.116	-30.767 ± 0.468	-22.543 ± 0.509	-25.347 ± 0.085	2.045 ± 0.241	0.111 ± 0.124
HS_20200717T165253	0.659 ± 0.101	1.157 ± 0.16	-23.591 ± 2.217	-28.424 ± 1.382	-21.079 ± 2.238	-24.596 ± 1.876	2.845 ± 0.228	0.143 ± 0.165
HS_20201229T165256	0.629 ± 0.039	1.12 ± 0.09	-24.331 ± 1.526	-30.445 ± 1.461	-21.291 ± 1.149	-24.986 ± 0.638	2.566 ± 0.227	0.184 ± 0.18
HS_20210109T165256	0.604 ± 0.011	1.11 ± 0.025	-24.011 ± 1.108	-31.464 ± 1.66	-21.64 ± 1.053	-25.638 ± 0.129	2.729 ± 0.2	0.34 ± 0.133
SL_20210316T165254	1.17 ± 0.001	1.555 ± 0.002	-25.307 ± 0.117	-29.781 ± 0.577	-23.19 ± 0.09	-25.359 ± 0.242	2.668 ± 0.198	0.263 ± 0.124
SL_20210327T165254	1.17 ± 0.001	1.563 ± 0.003	-25.6 ± 0.638	-30.125 ± 0.635	-23.931 ± 1.387	-25.429 ± 0.232	2.797 ± 0.201	0.264 ± 0.124
SL_20210407T165255	1.168 ± 0.001	1.561 ± 0.002	-25.256 ± 0.572	-29.516 ± 0.298	-23.204 ± 0.18	-25.264 ± 0.329	2.67 ± 0.198	0.207 ± 0.135
SL_20210418T165256	1.167 ± 0.002	1.551 ± 0.001	-25.238 ± 0.282	-29.656 ± 0.58	-23.207 ± 0.053	-25.359 ± 0.137	2.635 ± 0.196	0.25 ± 0.134
SM_20200329T165246	1.748 ± 0.004	2.958 ± 0.004	-26.104 ± 0.324	-30.568 ± 0.544	-24.808 ± 0.232	-25.051 ± 0.723	2.605 ± 0.19	0.23 ± 0.132
SM_20200409T165247	1.753 ± 0.005	2.952 ± 0.022	-26.227 ± 0.267	-30.237 ± 0.836	-24.801 ± 0.036	-25.347 ± 0.385	2.719 ± 0.192	0.244 ± 0.109
SM_20200420T165248	1.75 ± 0.003	2.962 ± 0.004	-26.716 ± 0.594	-30.642 ± 0.954	-24.122 ± 1.911	-25.135 ± 0.758	2.734 ± 0.193	0.225 ± 0.136
SM_20200501T165248	1.752 ± 0.004	2.966 ± 0.005	-26.661 ± 0.536	-29.764 ± 0.719	-23.991 ± 1.325	-25.16 ± 0.431	2.574 ± 0.189	0.176 ± 0.097

3.2 Equivalent Number of Looks (ENL)

The ENL analysis is typically performed over natural distributed homogeneous targets. In this analysis the test areas used for the analysis were in the Amazonas Rainforest, Antarctica Glacier and Sahara Desert (Sudan and Egypt). The SC dataset was in MGD processing mode, and the other acquisition modes in SSC mode. The ENL value for SSC should be close to 1, while the value for MGD depends on the multilook factor applied. Table 7 presents the number of SSC and MGD datasets for each analysed environment.

Table 7: The number of analyzed SSC and MGD scenes over the homogeneous targets; rainforest, glacier and desert.

Target	SSC	MGD (ScanSAR)
Rainforest	5	1
Glacier	2	2
Desert	4	0

The ENL analysis is performed using the SQT software, by manually choosing a sub-window containing homogeneous texture from the SAR backscatter image and applying the calculation of the ENL to the chosen window. Figure 7 presents an example of a chosen sub-window in a SL scene from the Sahara Desert.
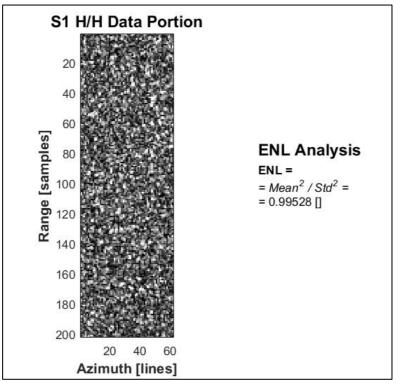

Figure 7. ENL analysis example for SL_20180913T034217_20180913T034218.

3.2.1 Rainforest

Rainforests are considered homogeneous targets, especially for X-band sensitive to tree canopies. In this analysis six PAZ scenes were available from the Amazonas Rainforest; one SC, three SM, one SL (dual-polarization) and one HS scene. Only the SC scene was processed to MGD, while all the rest were processed to SSC product type. Table 8 shows the calculated and the ideal ENL (number of looks) for the rainforest scenes. The table shows the average and the standard deviation of ENL values calculated from 5 sub-windows selected from each image.

Table 8: The average and the standard deviation of measured ENL from the rainforest, calculated from 5 sub-windows for each image, as well as the ideal ENL (number of looks) for each scene.

Image	ENL	Number of looks (az*rg)
SC_20180724T103235	5.413 ± 0.179	5.25

SM_20180729T104201	0.558 ± 0.013	1.00
SM_20180829T230505	0.422 ± 0.015	1.00
SM_20190111T102407	0.493 ± 0.075	1.00
HS_20180917T222156	0.669 ± 0.09	1.00
SL_20180917T222316 / VV	0.626 ± 0.026	1.00
SL_20180917T222316 / HH	0.631 ± 0.022	1.00

The derived ENL of the SC image was around 5.4, close to the ideal value of 5.25, which is the number of looks. The derived ENL for the SM, SL and SH was between 0.6 and 0.7, meaning lower than the ideal value of ENL=1 for SSC. The measured lower ENL in rainforests might be due to relatively non-homogeneous target with respect to the fine spatial resolution of the SM, SL and HS data.

3.2.2 Glacier

Glaciers are also homogeneous targets which enable the testing of ENL. Table 9 show the average and the standard deviation of the ENL measured in 5 sub-windows for each scene from the Glacier. The measured ENL of the SC MGD scenes is close to the number of looks, indicating correct processing of the SAR data. The measured ENL of the SM scenes is very close to the ideal value of ENL=1, which also indicates radiometrically correct processing of the data.

Table 9: The average and the standard deviation of measured ENL from the glacier, calculated from 5 sub-windows for each image, as well as the ideal ENL (number of looks) for each scene.

Image	ENL	Number of looks (az*rg)
SC_20190303T071204	7.911 ± 0.232	8.74
SC_20190423T051400	6.596 ± 0.088	6.52
SM_20180928T202612	0.993 ± 0.008	1.00
SM_20180930T071214	1.007 ± 0.006	1.00

3.2.3 Desert

For confirming the results of the ENL analysis for the relatively high resolution SM and SL data, we also tested the ENL in desert areas. Deserts are homogenous targets and have a relatively low backscatter due to smooth and dry soil. Hence, they are primarily used for assessing the contribution of noise in the SAR images (NESZ). However, due to the homogeneous texture of the desert images, they can also be utilized for assessing the ENL. PAZ data from the desert included two SM and two SL scenes (one of them dual polarization). Table 10 show the average and the standard deviation of the ENL measured in 5 sub-windows for each band from the Sahara Desert. All images have ENL values close to one, indicating correct radiometric processing of the SAR data.

Table 10: The average and the standard deviation of measured ENL from the desert, calculated from 5 sub-windows for each image, as well as the ideal ENL (number of looks) for each scene.

Image	ENL	Number of looks (az*rg)
SL_20180924T034217 / HV	0.976 ± 0.012	1
SL_20180924T034217 / HH	0.944 ± 0.021	1
SL_20180913T034217	0.96 ± 0.033	1
SM_20181122T161007	0.958 ± 0.028	1
SM_20181111T161010	0.952 ± 0.025	1

3.3 Noise Equivalent Sigma Zero

One of the most essential quality indicators in SAR is the noise equivalent sigma zero (NESZ), showing the contribution of noise in the observed backscatter. Weaker NESZ is an indication of higher quality SAR data, because targets with relatively low backscatter can be identified with less noise disturbance. The NESZ is assessed using the SQT by manually extracting and plotting a range profile of the sigma nought (σ^0) backscatter from low backscatter areas. The minimum of the graph can be considered the NESZ value, assuming that the contribution of the target itself to the backscatter power is negligible. For dual polarization images the cross-pol band was preferred over the co-pol band. Figure 8 shows an example of a range profile extracted from one of the SM images over the Pacific Ocean.
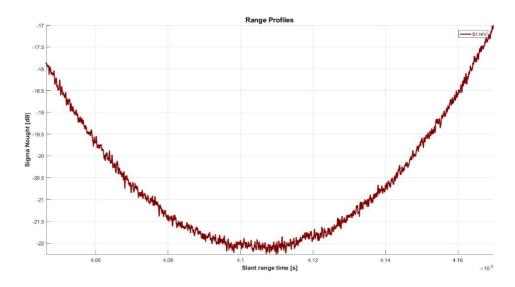

Figure 8: A range profile extracted from a SM scene over the Pacific Ocean acquired in 25.10.2018, for measuring the NESZ.

Table 11 shows the NESZ values for each product type provided in the PAZ documentation. The given NESZ values are considered the worst case within the whole full performance incidence angle ranges. The measured NESZ of the test datasets should therefore be lower than the values in Table 11.

Table 11: NESZ of different products provided in the PAZ documentation.

Product type	Polarization	NESZ [dB]
Wide ScanSAR	Single	-24
ScanSAR	Single	-18
Stripmap	Single	-16.8
Stripmap	Dual	-18.5
Spotlight	Single	-18.7
Spotlight	Dual	-16.5
HR Spotlight	Single	-16.2
HR Spotlight	Dual	-16.8
Staring Spotlight	Single	-19

Table 12 shows the derived NESZ for the scenes acquired from water surfaces; two SM and one HS scenes from the Pacific Ocean, and one SC scene from Lake Michigan, USA. The NESZ of all test scenes is at least 2 dB lower than the provided values. Especially the SM images show very low NESZ, more than 5 dB lower than the defined values in the documentation (Table 11).

Table 12: Measured NESZ for the Pacific Ocean (HS and SM) and Lake Michigan (SC) sites.

Image	NESZ (dB)
SC_20181025T120434	-20
HS_20181026T150743 / HV	-19.7
SM_20181027T025940 / HV	-23.36
SM_20181025T033317	-22.17

Table 13 shows the derived NESZ for the scenes acquired from the desert; two SM and two SL scenes. The SL dual-pol scene (acquired at 24.9.2018) shows NESZ somewhat higher than the defined -16.5 value, and the SL single-pol scene (acquired at 13.9.2018) shows slightly higher NESZ compared to the -18.7 dB provided in the PAZ documentation. In contrary, the SM scenes show NESZ values more than 2.5 dB lower than the defined values in the documentation. Generally, based on the analysed data from the low backscatter areas, the PAZ data shows low noise levels over the test areas, indicating good quality of images relative to the stated quality values.

Table 13: Measured NESZ for the Sahara Desert sites.

Image	NESZ (dB)
SL_20180924T034217 / HV	-15.9
SL_20180913T034217	-18.4
SM_20181122T161007	-21.48
SM_20181111T161010	-19.66

3.4 Antenna Elevation Pattern

The observed values need to be corrected for changes caused by the beam elevation angle in the range direction. A pre-defined antenna elevation pattern (AEP) is used by the data provider for compensating the contribution of the elevation angle to the measured gain. In this section we assessed whether the AEP correction was applied correctly on the data. The images were analysed by averaging the backscatter in azimuth direction and extracting range profiles of the averaged backscatter in slant range time units for SSC and in ground range distance for MGD products. The backscatter was then normalized by the inverse of the average measured backscatter. The analysis was performed on the Rainforest scenes, where the noise component can be considered negligible (very low) compared to the target backscatter level. Gamma nought (γ^0) backscatter was chosen because it is independent of the incidence angle with the ground surface. Ideally, the normalized γ^0 range profiles should be horizontal, with a value of zero dB along the x-axis.

Data acquired from the Amazonas Rainforest included one SC, three SM, one SL and one HS scene. In the PAZ documentation there was no reference values or explanation on how the AEP correction of the products was performed. Therefore, the measured results are evaluated on the basis of common quality level.

The figures below (Figure 9 - Figure 14) show the normalized antenna pattern with respect to the slant range time or ground range distance, extracted from the analysed SAR images. The profiles show similar backscatter for the different elevation angles, with backscatter trend change of less than 0.5 dB from near to far range. Some spikes can be seen in the HS (Figure 9), SL (Figure 10) and in two out of the three SM scenes (Figure 11, Figure 13), due to exceptional targets on the

ground, such as rivers, forest cuts or roads. However, the general trend with respect to the elevation angle is nearly flat in all cases. Hence, based on our analysis, the AEP correction applied by the data provider can be considered accurate for all acquisition modes.
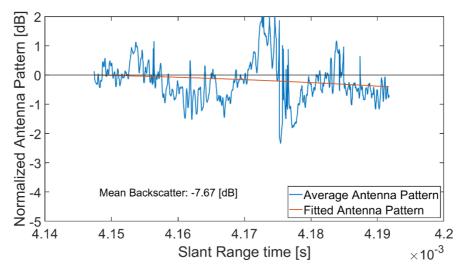

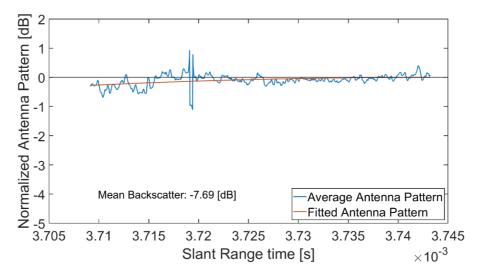**Figure 9: AEP for the HS scene acquired at 17.9.2018 from the rainforest.**

Figure 10: AEP for the VV-polarization band of the SL scene acquired at 17.9.2018 from the rainforest. The HH-polarization band has a very similar profile.
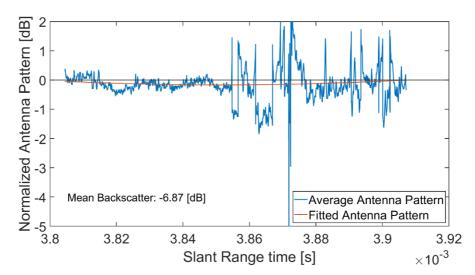
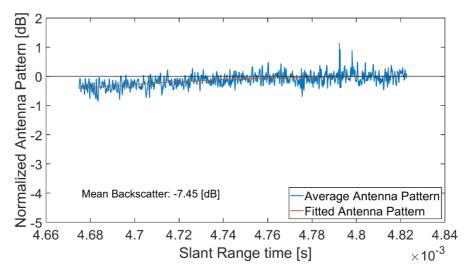**Figure 11: AEP for the SM scene acquired at 29.7.2018 from the rainforest.**

Figure 12: AEP for the SM scene acquired at 29.8.2018 from the rainforest.
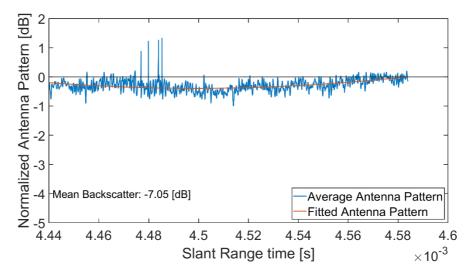

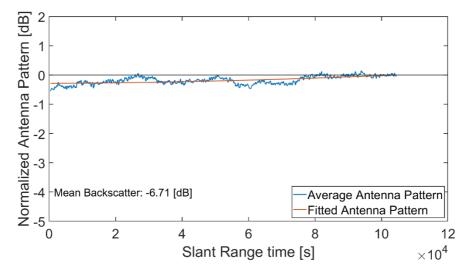**Figure 13: AEP for the SM scene acquired at 11.1.2019 from the rainforest.**

Figure 14: AEP for the SC scene acquired at 24.7.2018 from the rainforest.

3.5 Processing in SNAP

For assessing the accessibility and usability of the PAZ data products, the scenes from Argentina were processed in the freely available SNAP version 8.0 distributed by ESA. The processing included basic SAR operations, such as calibration to sigma zero, georeferencing including compensation of the effect of ground elevation using the Copernicus 30 m DEM (Terrain Correction), and speckle filtering. The products from the Mendoza Province, Argentina, were processed to GeoTIFF file format in the UTM grid. The SC MGD data were filtered with a "Gamma Map" speckle filter using a window size of 5 x 5 pixels, and the SM SSC data were multilooked to a 2 x 2 m cell size and filtered with a "Gamma Map" speckle filter using a window of 7 x 7 pixels. The processing in SNAP was successfully completed for all tested four products. Figure 15 is a screenshot from the SNAP view of the location of the SAR scenes over a background satellite image. Figure 16 shows a sub-area of the SM scenes, and Figure 17 shows a sub-area of the processed SC scenes.

Figure 15: SNAP view of the location of the SC and SM scenes from the Mendoza Province in Argentina over a background map.
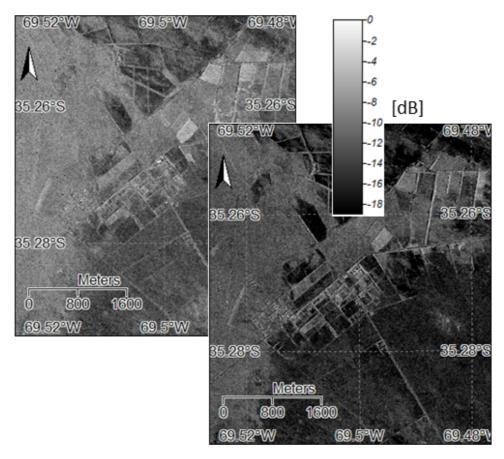

Figure 16: SM backscatter images processed in SNAP. The scenes were acquired at the 24.11 (top) and the 22.12 (bottom) 2018 from the village of La Junta, Mendoza Province, Argentina.
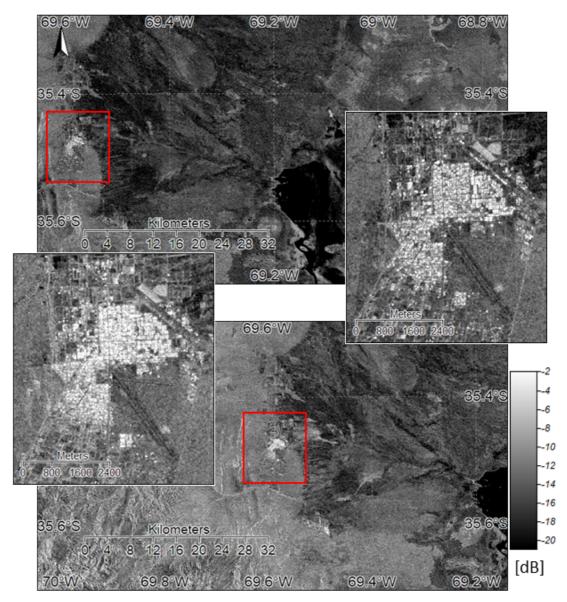
Figure 17: SC backscatter images processed in SNAP. The scenes were acquired at the 25th (top) and the 19th (bottom) of Sep 2018 around the town of Malargue, Mendoza Province, Argentina. The smaller images are a zoom in of the SC scenes on the town of Malargue.

4. CONCLUSIONS

An assessment of the available PAZ documentation and the PAZ data was performed by FMI. The documentation was found to be overall in a basic level. The openly available "SAR Level 1b Product Format Specification for PAZ SAR Processor" (RD-1) and "PAZ Image Product Guide" (RD-2) provided most of the necessary information regarding the data products, characteristics, and uncertainty. The "End User License Agreement" (RD-3) pointed out the terms of use. No other documentation was provided by Hisdesat. Hence, more detailed information describing the methods used for sensor calibration or for deriving the stated uncertainty values was not available.

An independent data analysis of test datasets was performed by FMI using mainly the SQT software. In this work we evaluated the ScanSAR (SC), StripMap (SM), Spotlight (SL) and High Resolution Spotlight (HS) acquisition modes. The relevant parameters describing the SAR data quality were retrieved and compared with the corresponding values provided by Hisdesat in the available PAZ documentation. The measured IRF quality metrics were found to be in line with the values provided by Hisdesat. These values include the spatial resolution and the geolocation accuracy. The PSLR and ISLR were not given in the PAZ documentation, but instead, the used alpha value in the applied Hamming window filter was expressed. The PSLR and ISLR were found to be in line with the theoretical values in azimuth direction, but few decibels higher in the range direction. NESZ was found to be similar or lower (better) than the values provided in the PAZ documentation. The measured ENL in rainforests was typically less than the expected value of ENL=1 for the SSC data. This might be related to the difficulty in finding entirely homogeneous regions in the relatively high-resolution data examined from the rainforest. Instead, the ENL in the Glacier and the Desert sites was very close to the ideal value of one. The ENL of the SC MGD data was close to the ideal values of the number of looks. The gamma nought backscatter (γ^0) profile was found to be relatively flat with respect to the elevation angle in the rainforest scenes, indicating an accurate correction of the AEP by the data provider. The PAZ data was successfully processed in the publicly available SNAP software, including basic SAR operations such as calibration, geometric correction, and speckle filtering.

Based on the assessment described in this document, the PAZ SAR data have been found to be of good quality relative to the uncertainty values stated by the data provider. However, information provided by Hisdesat in the available documentation covers only basic information.

REFERENCES

RD-1   SAR Level 1b Product Format Specification for PAZ SAR Processor (https://www.hisdesat.es/wp-content/uploads/2019/10/PZ-DLR-ID-3003_SAR_Level_1b_Product_Format_Specification.pdf)

RD-2   PAZ Image Product Guide (https://www.hisdesat.es/wp-content/uploads/2021/06/PAZ-HDS-GUI-001-PAZ-Image-Products-Guide-issue-2.pdf)

RD-3   End User License Agreement (https://www.hisdesat.es/wp-content/uploads/2019/10/EULA_PAZ_EN_v1.0.pdf)